Journal of Solid State Chemistry 183 (2010) 2886–2894

Contents lists available at ScienceDirect

Journal of Solid State Chemistry

journal homepage: www.elsevier.com/locate/jssc

Investigation of structural, morphological, luminescent and thermal properties of combusted aluminium-based iron oxide

S.S. Shinde, K.Y. Rajpure *

Electrochemical Materials Laboratory, Department of Physics, Shivaji University, Kolhapur 416004, India

ARTICLE INFO

Article history:
Received 20 June 2010
Received in revised form
16 September 2010
Accepted 27 September 2010
Available online 1 October 2010

Keywords:
Combustion
Iron oxide
Morphology
XPS
PL
Thermal conductivity
Complex impedance

ABSTRACT

Nanocomposites of aluminium integrated hematite α-Fe_2O_3 are synthesized by combustion route using aqueous solutions of AR grade ferric trichloride and aluminium nitrate as precursors. The influence of aluminium incorporation on to the morphology, XPS, photoluminescence and thermal properties has been investigated. The FESEM and AFM micrographs depict that the samples are compact and have homogeneously distributed grains of varying sizes ($\sim$20–60 nm). Chemical composition and valence states of constituent elements in hematite are analyzed by XPS. In room temperature photoluminescence (PL) study, we observed strong violet emission around 436 nm without any deep-level emission and a small PL FWHM indicating that the concentrations of defects are responsible for deep-level emissions. The specific heat and thermal conductivity study shows the phonon conduction behavior is dominant. We studied interparticle interactions using complex impedance spectroscopy. We report a new potential candidate for its possible applications in optoelectronics and magnetic devices.

1. Introduction

The synthesis of nanocomposites comprising nanoscale materials with different physico-chemical properties has been investigated widely in efforts to design advanced materials with enhanced properties [1]. During last decade a large number of investigations have been focused on iron oxide based nanoparticles for their potential applications in ferrofluids [2], magnetocaloric refrigeration [3] and biotechnology. Besides, these materials offer several potential biomedical applications, specifically, for magnetically controlled drug delivery [4], magnetic resonance imaging [5], tissue repair, immunoassay, detoxification of biological fluids [6] and as nanosensors [7]. Recent interest in this area has led to colloidal iron oxide particles for their better usage in biomedicine [8]. By selecting appropriate constituent elements, the associated crystals and derived electronic structures of oxides can be altered by manipulating the delicate equilibrium in the bonding requirements of a lattice, thus leading to a wide spectrum of physical properties. Their functionalization with Al has demonstrated vast potential in catalysis [9] and biotechnological applications, namely protein separation [10], cancer diagnosis [11], as biosensors and bioactuators [12]. In most of the biological applications, magnetic properties of these particles, and in particular superparamagnetism, have been considered to contribute significantly [13]. The incorporation of metal/metal ions into iron oxide(s) also results in the formation of 'delafossites' [9]. These materials have found utility in electric switch contacts, soldering, increasing high-density storage capacity [14], thermoelectric devices [15,16], field emission displays (FEDs) [17], ozone sensors [18], photocatalytic hydrogen generators [19], magnetic semiconductors for spintronics [20] and optoelectronic technology [21,22]. In the literature we did not come across any report on the synthesis of aluminium-based iron oxide.

The present work reports a new method for the synthesis of nano-sized aluminium iron oxide nanocomposite with a narrow size distribution by interacting colloidal α-Fe_2O_3 with aluminium particles. The resulting composite system has been characterized by using XRD, FESEM, AFM, XPS, PL, impedance and hysteresis techniques. Thermal measurements were performed for the study of specific heat and thermal conductivity under different experimental conditions. Also we have studied an interparticle interactions using complex impedance spectroscopy.

2. Experimental

The aluminium-added iron oxide samples were prepared by a combustion route using AR grade equimolar (0.1 M) ferric trichloride ($FeCl_3$) and aluminium nitrate ($Al(NO_3)_2$ of s. d. fine Ltd, Mumbai, with 98.6% and 99.5% purity. The preparation conditions

* Corresponding author. Fax: +91 231 2691533.
E-mail address: rajpure@yahoo.com (K.Y. Rajpure).

0022-4596/$ - see front matter © 2010 Elsevier Inc. All rights reserved.
doi:10.1016/j.jssc.2010.09.035

were carefully controlled. A mixture of precursors in atomic proportion was taken in to a Pyrex dish and melted by heating at 80 °C. Then appropriate amount of fuel glycine was added in the mixture. After evaporation of the water content, the mixture ignited to combust with a flame, giving voluminous and foamy samples. The aluminium doping (in starting solution) was varied from 0 to 20 at%. The synthesized powder was annealed at 350 °C. These compositions were further mixed with polyvinyl alcohol as a binder and pressed into pellets of 15 mm diameter and 2–3 mm thickness using a hydraulic press (5 ton for 5 min). Then prepared pellets were annealed for 400 °C for 1 h for the removal of binder.

The morphological characterization of the samples was studied by using field emission scanning electron microscopy (FESEM, Model: JSM-6701 F, Japan). The surface topography of samples was further analyzed from AFM images taken by means of the atomic force microscopy (AFM, Digital Instrument, Nanoscope III) operated at room temperature. AFM images were collected in contact mode on a molecular imaging system using a silicon nitride cantilever. The chemical composition and valence states of constituent elements were analyzed by using X-ray photoelectron spectroscopy (XPS, Physical Electronics PHI 5400, USA) with monochromatic Mg–$K\alpha$ (1253.6 eV) radiation source. Photoluminescence (PL) spectra were obtained using a closed-cycle liquid helium cryogenerator (APD, SH-4, USA), a spectrometer (f=0.5 m, Acton Research Co., Spectrograph 500i, USA) and intensified photodiode array detector (Princeton Instrument co., IRY1024, USA). All spectra were measured at room temperature with an Ar^+ ion laser as a light source using an excitation wavelength of 325 nm. The specific heat capacity and thermal conductivity was measured by C-T meter made by Teleph Pvt. Ltd., France. The impedance parameters namely Z' and Z'' for all the samples were measured at various temperatures in the frequency range 20 Hz–1 MHz using a precision LCR meter bridge (model HP 4284 A). Magnetic properties were studied using hysteresis loop tracer (Magneta B–H loops tracer) at a maximum applied field of 4 KOe.

3. Results and discussion

3.1. Structural analysis

Fig. 1 shows X-ray diffraction patterns of the undoped and typical 10 at% Al added iron oxide samples. From these patterns, it is seen that synthesized samples are of hematite (α-Fe_2O_3) phase. The samples are polycrystalline and fit well with the rhombohedral crystal structure having space group $R3$ (148). These samples of α-Fe_2O_3 are in correspondence with 03-0800 in Powder Diffraction File (PDF) collected by the Joint Committee on Powder Diffraction Standards (JCPDS). For the 10 at% Al:Fe_2O_3 sample, the diffraction angle of the (202) peak is almost in agreement with the Fe_2O_3 bulk single crystal, implying that no evident residual stress or inclusion-induced lattice distortion has developed in the Fe_2O_3 sample due to Al incorporation [23,24]. Some weak reflections such as (012), (104), (110), (006), (113), (202), (024) and (116) have also been observed but with small intensities. After addition of aluminium into the host lattice, intensity of all reflections goes on decreasing.

The average crystallite size is calculated employing Scherrer's equation

$$D = \frac{0.9\lambda}{\beta \cos\theta} \quad (1)$$

where D is the crystallite size, λ is wavelength of X-ray, β is full width at half maximum in radian, and θ is Bragg's angle. The average crystallite size is of the order of 18 and 12 nm for undoped and 10 at% aluminium added samples, respectively.

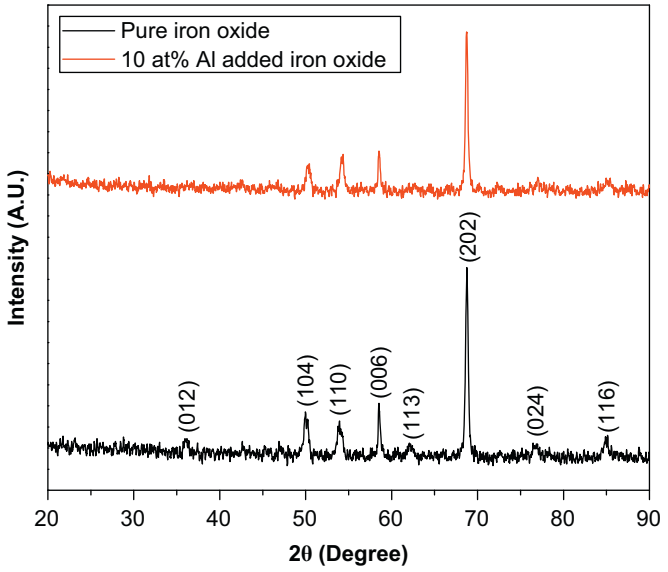

Fig. 1. X-ray diffraction patterns of undoped and typical 10 at% Al-added iron oxide samples

3.2. Surface morphological study

Fig. 2(a)–(e) shows the FESEM images of aluminium added (0–20 at% doping concentration) iron oxide samples. The micrographs depict that the samples are compact and homogeneous distribution of grains with varying sizes have been observed. The pure iron oxide sample shows the agglomerated highly dense, compact and homogeneous structure. The large value of the grain size observed by SEM may be explained by the tendency of the small grains to aggregate to the big grains in the sample. Apparently, the Al-doping affects the grain size leading to a grain width reduction, as clearly observed in Fig. 2(b)–(e). As the doping concentration increases from 0 to 10 at%, compactness of grains and grain size decreases and number of grains increases. From the images, it is confirmed that the powder samples are converting from the microcrystalline to nanocrystalline phase. Average grain size observed for the all samples are in the range 15–55 nm. Therefore, it can be concluded that the morphology and grain size affects due to doping concentration. There are two possibilities associated with the phenomena. One is the effect from outside and the other from inside. It is known that, the oxygen and vapor in the air would have big effect on the morphology. When there is an exchange of oxygen between grains and air, the collapse may happen. We tend to agree with the second mechanism that the collapse is probably due to the strain release of crystallites due to high temperature. The formation of 3D crystallites is mainly governed by surface energy, elastic strain and surface diffusion kinetics. Theoretically, small regions of high strain will evolve as grooves or pits if, strain is not homogeneously relieved during the growth [25]. Therefore, we can assume that the uneven component distribution of Fe_2O_3 grow at relatively low concentrations could result in local sites with high strain. As a result, the depositing materials diffused away from these high-strain sites.

Fig. 3(a,b) shows two- and three-dimensional atomic force microscopy (AFM) images of pure and optimized 10 at% aluminium added iron oxide powder samples. The images were recorded on $1 \times 1\ \mu m^2$ planar in contact mode at the scan rate of 10.17 Hz. Uniformly distributed agglomerated grains of varying sizes are seen. It is seen that grain size decreases after incorporation of aluminium. One can see that by increasing the number of thermal treatments grains of regular shapes develop